Lamellar Structures of Anionic Poly(amido amine) Dendrimers with Oppositely Charged Didodecyldimethylammonium Bromide

Xingfu Li, Toyoko Imae,* Dietrich Leisner, and M. Arturo López-Quintela†

Research Center for Materials Science, Nagoya University, Chikusa, Nagoya 464-8602, Japan

Received: April 8, 2002; In Final Form: September 6, 2002

The lamellar structures of anionic poly(amido amine) dendrimers possessing carboxylate terminal groups at half-generations G = *n*.5 (G2.5 and G4.5) with the cationic surfactant didodecyldimethylammonium bromide (DDAB) were investigated by small-angle X-ray scattering (SAXS) at 25 °C. The incorporation of dendrimers into the lamellar liquid crystals, at DDAB concentrations in the range of 4∼30 wt %, results in the transition from a monophasic lamellar structure (L_α) to biphasic lamellar mixtures (L_α and L_α^D), at similar 2[DDAB]/[−COONa] ratios for the two dendrimers with the later and earlier generations (56 for the G4.5 dendrimer and 62 for the G2.5 dendrimer). The L_α structure consists of DDAB bilayers and dendrimer molecules doped into the water domains. The oppositely charged dendrimer preferably sticks to the DDAB bilayers, resulting in the decrease in the domain size of the wide spaced L_α structure with increasing the dendrimer concentration. In the narrow spaced L_α^D structure, monolayers of collapsed dendrimers are adsorbed tightly between the DDAB bilayers. The thicknesses of the dendrimer monolayers are found to be 4.2 nm for the G4.5 dendrimer and 3.0 nm for the G2.5 dendrimer. These values are smaller than the diameters of the corresponding dendrimers found in aqueous solution. It is also deduced from Gaussian fits of SAXS patterns that the G4.5 dendrimer can form more ordered L_α^D structures with domain sizes larger than those of the G2.5 dendrimer, due to the stronger electrostatic interaction between the cationic surfactants and the oppositely charged dendrimers with terminal groups located at shorter distances.

Introduction

The poly(amido amine) (PAMAM) family of dendrimers is a widely investigated group of dendritic polymers possessing branched repeating units radially attached to a central core. The controlled synthesis of dendrimers produces structures with nanoscopic size and well-defined composition and constitution.[1−6] When the branches at the exterior surface of PAMAM dendrimers are terminated at half-generation (G ≡ *n*.5) by forming carboxylate groups with sodium gegenions, molecular simulation of the PAMAM dendrimer structure has revealed a change in the dendrimer morphology occurring after the 3.5 generation.[1,3] The so-called earlier generation dendrimers (G ≤ 3.5) have an open structure, whereas the later generation dendrimers (G > 3.5) present a densely packed exterior structure.[1,2,4]

The interactions of dendrimers with ionic surfactants in aqueous solutions are of fundamental relevance to industrial and biological processes.[1,4] For instance, the structure of biological cell membranes, the transport of materials within biological systems, and several petrochemical and pharmaceutical industrial processes are based mainly on the interactions between natural or synthetic polymers and surfactant aggregates in the form of micelles, vesicles, bilayers, and multilayers. The interactions and complexes formed between dendrimers and surfactants have been the subject of a range of investigations in recent years. The complexes with dodecyltrimethylammonium bromide (DTAB), in particular, were investigated using the fluorescence probe in Gn.5 PAMAM dendrimer solutions.[1,3] Caminati et al. studied the formation of both primary (noncooperative) and secondary (cooperative) binding of DTAB at the dendrimer/water interface as a function of DTAB concentration and dendrimer generation. This study provided a reference point for the research on the binding interactions and aggregation processes of cationic surfactants in the presence of n.5 dendrimers with different generations.

While many investigations were made on the supramolecular structures and interactions of dendrimers at low surfactant concentrations,[1−6] relatively little has been reported at high surfactant concentrations.[7,8] Friberg et al.[7] reported the formation of liquid crystal by octanoic acid and polyethyleneimine dendrimer. In the liquid crystal, surfactants formed ionic pairs with amino terminals of dendrimer. Baars et al.[8] investigated the scattering displays based on the addition of dendrimers to continuous liquid crystals for the development of an electro-optical switch, but they did not discuss the morphology of hybrid liquid crystalline structures. Many studies on the influence of polymers on the lamellar structure by the conflicting demands of polymer conformation and liquid crystalline ordering confirm that electrostatic interactions play a decisive role.[9−11] Keeping these facts in mind, we initiated studies on the structures and interactions of dendrimers in the lamellar phase.

In the present work we investigated the incorporation of PAMAM dendrimers with carboxylate terminal groups into the lamellar phase in the system didodecyldimethylammonium bromide (DDAB)−water. Two kinds of dendrimers, at G = 2.5 and 4.5, were selected as representatives of the earlier and later generations. The structural changes were analyzed by means

* Corresponding author: Toyoko Imae, Research Center for Materials Science, Nagoya University, Chikusa, Nagoya 464-8602, Japan. TEL: +81-52-789-5911. FAX: +81-52-789-5912. E-mail: imae@nano.chem.nagoya-u.ac.jp

† Visiting professor of the Research Center for Materials Science, Nagoya University, Japan. Present address: Facultad de Química, Universidad de Santiago de Compostela, E-15782, Santiago de Compostela, Spain.

10.1021/jp020926o CCC: $22.00
Published on Web 11/01/2002

TABLE 1: Structural Characteristics of PAMAM Dendrimers Possessing Terminal Carboxylate Groups[1,2,14,18]

generation	molecular weight	diameter[a] (nm)	terminal groups	shape and structure
1.5	2935	2.8	16	an asymmetric shape
2.5	6267	3.9	32	open structure
3.5	12931	4.8	64	
4.5	26258	5.9	128	a nearly spherical shape
5.5	52912	7.1	256	a densely packed exterior structure

[a] Determined by size exclusion chromatography (SEC) in water.

of small-angle X-ray scattering (SAXS). The present investigation addresses the following subjects. (1) The lamellar structures of DDAB at high concentrations. In this respect, the effect of DDAB concentration on the thickness of water and DDAB layers and cross-sectional area of hydrophilic heads of DDAB is investigated. (2) The lamellar structures with doped PAMAM dendrimers. The lamellar structure is investigated as a function of dendrimer concentration, dendrimer generation, and surfactant concentration. (3) The electrostatic interactions of dendrimers with surfactants. The investigation is focused on the relationship between the lamellar structure and the electrostatic interaction of surfactants with dendrimers at the earlier and later generations. (4) The domain sizes of lamellar structures. Schematic models will be proposed for the lamellar structures of dendrimers and surfactants. Such models can be used to explain the relations between the variation in the domain size and the microstructure of hybrid liquid crystals.

Experimental Section

Materials. The methanol solutions of the G2.5- and G4.5-PAMAM dendrimers were obtained from Aldrich Chemical Co. Each dendrimer consists of a tetra functional $>NCH_2CH_2N<$ core and $-CH_2CH_2(C{=}O)NHCH_2CH_2N<$ repeating units, and is terminated at the final generation with carboxylate groups (see the details shown in Table 1).[12] Methanol solutions of dendrimers were dried in a nitrogen atmosphere, and 1% aqueous solutions of dendrimers were prepared. The Milli Q water used was purified by a Millipore filter (with the pore size at 0.2 μm). DDAB, with purity of analytical grade, was purchased from Tokyo Kasei Kogyo Co., Ltd., and used without further purification.

Sample Preparation. Samples were prepared individually by weighing appropriate amounts of aqueous dendrimer solution, water, and DDAB into glass tubes. The DDAB concentration in wt %, W_S = DDAB/(DDAB + Gn.5 + water) × 100, was fixed at 5, 10, 20, and 25%. The dendrimer concentration in wt %, W_D = Gn.5/(DDAB + Gn.5 + water) × 100, was increased from 0 to 1.0%. To attain the good homogeneity of the mixtures, a vortex mixer was used for rather dilute samples, whereas concentrated samples were mixed in a supersonic bath at around 40 °C. These samples were kept at 25 °C in a water bath controlled by a thermostat from several hours to several weeks until equilibrium was attained. The formation of liquid crystals was detected with a crossed polarizer. The type of liquid crystals was further identified with SAXS.

SAXS. X-ray measurements of the samples were performed at 25 ± 0.1 °C with a Rigaku instrument (SAX-LPB) using multilayer confocal max flux (CMF) miller optics. The X-ray radiation source (CuK_α, λ = 0.154 nm) was operated at 45 kV and 80 mA. An imaging plate was used as a detection system for the SAXS measurements. The sample-to-detector distance was set at 1 m. The X-ray exposure time was fixed at 24 h for each sample of liquid crystals. The scattering vector amplitude q range covered was from 0.2 to 3.5 nm^{-1} with $q = (4\pi/\lambda)\sin(\theta/2)$, θ being the scattering angle. The experimental data were corrected for background scattering. The smearing effect was considerably low for the pinhole collimator.

The lamellar structure consists of surfactant bilayers and water domains. The thickness of the bilayer, i.e., twice as much as the thickness of the DDAB layer, d_S, can be expressed by[13]

$$2d_S = \phi_S d_1 \tag{1}$$

where d_1 ($= 2\pi/q_{max}$) is the interlayer spacing of the lamellar structures measured by SAXS, and ϕ_S the volume fraction of surfactant in the system. The effective cross-sectional area of the hydrophilic head of DDAB, a_S, and the thickness of the water domain, d_W, can be expressed as

$$a_S = \frac{V_S}{d_S N_A} = \frac{2V_S}{\phi_S d_1 N_A} \tag{2}$$

$$d_W = d_1 - 2d_S = (1 - \phi_S)d_1 \tag{3}$$

where V_S is the volume of the surfactant molecule, and N_A the Avogadro's number. The density values of DDAB, water, and dendrimer for calculation of V_S and ϕ_S are 0.962, 0.997, and 1.300 g/cm^3, respectively, at 25 °C.[14,15]

Domain Size Determination. Small-angle X-ray diffraction patterns are fitted to Gaussian profiles in the q range of the mean peak position.[16] From this fitting procedure, the following peak parameters are extracted: position, area, height (intensity), and full width at half-maximum (fwhm). A baseline subtraction was done before fitting the SAXS patterns. When the overlapping of two or three peaks is present, two or three Gaussian profiles are used to consider the contribution of the closest reflections to the main peaks. Taking two G4.5-containing samples at W_S = 10 and 20% as typical examples, two or three peaks were clearly separated, as shown in Figure 1.

The average domain size, D_{hkl}, was determined by applying the Debye−Scherrer formula to the first-order peak:[16]

$$D_{hkl} = \frac{2\pi k}{\omega} \tag{4}$$

where k (= 0.9) is a nondimensional shape factor and ω the integral breadth (in nm^{-1}). The ω is calculated by dividing the integrated peak area by the peak intensity.

The method is valid for estimates of the minimum average domain size rather than exact measures, unless the measured fwhm is considerably larger than the fwhm of the beam divergence (here 0.035 nm^{-1}) and the amplitude of layer undulations is smaller against the layer spacing than the fwhm against q_{max}, so that all peak broadening can be attributed to the limited number of interfering planes.

Results

Lamellar Structures in the DDAB−Water System. The phase behavior for the binary system DDAB−water at 25 °C is shown in Figure 2a.[15,17] DDAB is a highly insoluble surfactant, forming two lamellar liquid crystalline phases, a concentrated one at W_S = 83∼91% and a dilute one at W_S = 4∼30%. Below W_S = 3%, the amphiphile forms a lamellar dispersion, where different types of vesicular structures were identified (uni-, bi-, and multilamellar vesicles).[17]

To mimic the biological system of protein and cell membrane, we focused our investigation only on the structure of the dilute lamellar liquid crystalline phase at W_S = 4∼30%. We obtained two-dimensional (2D) SAXS patterns of the liquid crystals of

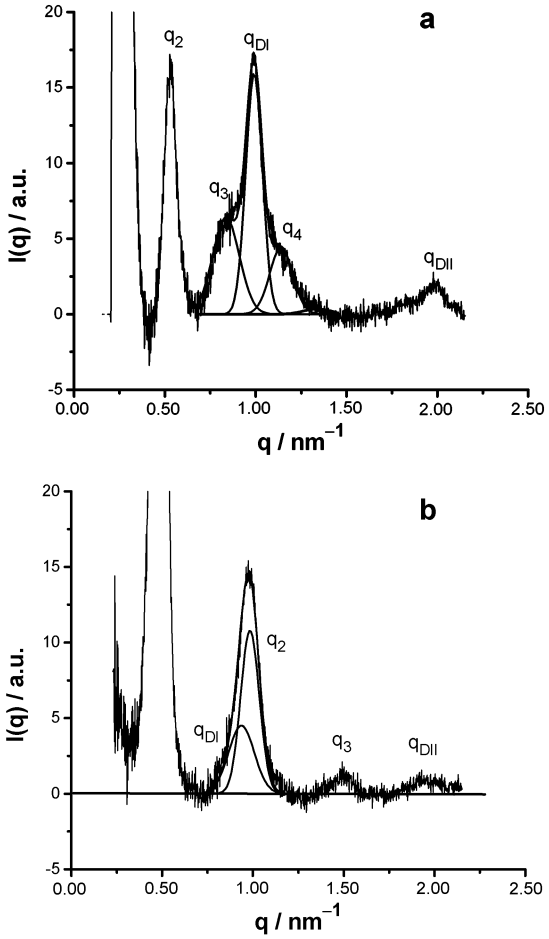

Figure 1. Typical Gaussian fits of the Bragg peaks of lamellar patterns for the DDAB−G4.5−water system. (a) $W_D = 0.412\%$ and $W_S = 10\%$, (b) $W_D = 0.393\%$ and $W_S = 20\%$.

DDAB, with sharp diffraction rings. For easier comparison of all the scattering data, the 2D SAXS patterns were azimuthally integrated and converted to one-dimensional $I(q)$ profiles along the radial coordinate. The SAXS profile of the sample at $W_S = 10\%$ (refer to the curve at $W_D = 0$ in Figure 3a) explicitly shows five diffraction peaks at $q = 0.268$, 0.541, 0.814, 1.09, and 1.36 nm^{-1}. The location of these peaks is in the ratio of 1:2:3:4:5 and confirms a lamellar structure.

The interlayer spacing of the lamellar structure (d_1) was measured by SAXS at DDAB concentrations from 4 to 30%. According to eqs 1−3, the thickness of the water domain (d_W) and DDAB layer (d_S) and the cross-sectional area of the hydrophilic head of DDAB (a_S) were calculated and shown in Figure 2b. The values of d_1 and d_W increase, and the values of a_S and d_S, on the other hand, remain almost constant with an increase in $(100 - W_S)/W_S$ along the dilution pathway from $W_S = 30$ to 4%. The values of d_S and a_S are 1.2 and 0.67 nm^2 respectively, suggesting that the bilayer structure of DDAB is not changed. Only the thickness of the water domain between the bilayers is gradually increased upon the dilution pathway in the lamellar structure region, as it is seen in the left part of Figure 4 without consideration for the dendrimers doped in the water domain.

Lamellar Structures Containing the G4.5 Dendrimer. *1. $W_S = 10\%$.* To investigate the structures and interactions of dendrimers with DDAB, which are dependent on the weight ratio between the dendrimers and the bilayers, we change the dendrimer concentration and dendrimer generation. Figure 3 shows plots of $I(q)q^2$ versus the scattering vector q with

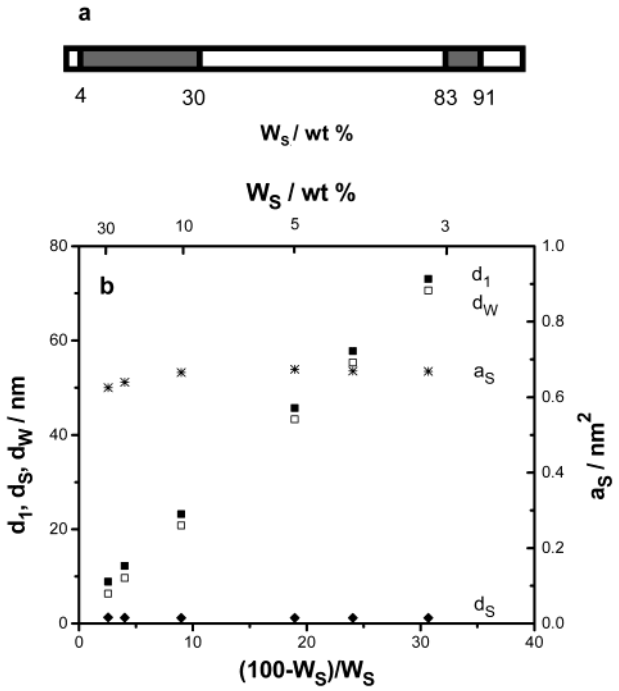

Figure 2. (a) Phase behavior for the system DDAB−water at 25 °C. Open areas correspond to the two-phase regions and shaded areas to the lamellar phase regions. (b) Spacings of the lamellar structure and cross-sectional areas of the hydrophilic head of DDAB as a function of $(100\text{-}W_S)/W_S$.

increasing the dendrimer concentrations for the different dendrimer systems at $W_S = 10$ and 20%. Although $I(q)$ versus q plots were used for the Gaussian fitting, as shown in Figure 1 and Table 2, we found that, with the plot of $I(q)q^2$ versus q, it is much easier to determine the position and intensity of the peaks at high q values.

It can be seen from Figure 3a that the DDAB phase at $W_S = 10\%$ shows a high ordered lamellar structure. With the addition of the G4.5 dendrimer to this lamellar structure, the intensity of the second- and third-order peaks decreases, and the position of the fourth-order peaks could only be resolved unambiguously at $W_D = 0.057\sim0.100\%$, showing a lamellar structure with a q ratio of 1:2:3. The small deviations from the expected peak positions were within the experimental error limit. At $W_D = 0.153\%$, the third-order peak became broadened and a new peak, q_{DI}, appeared at $q = 0.91$ nm^{-1}, which is far away from the position of the fourth-order peak at $q = 1.08$ nm^{-1}, showing the formation of a new structure. When $W_D = 0.195\%$, the broad peak was clearly split into two components and it reveals the coexistence of two structures. The intensity of the q_{DI} peak increased with an increase in the dendrimer concentration from 0.195 to 0.412%, and the location of these peaks shifted slightly toward high q values. The second-order peak, q_{DII}, of the second structure mentioned above could also be resolved unambiguously. The locations of these new peaks, shown in Figures 1a and 3a, support the validity of q_{DI}:$q_{DII} = 1{:}2$ at $W_D \geq 0.153\%$, indicating the formation of the second lamellar structure.

The lamellar structure of DDAB consists of bilayers of DDAB and domains of water. The trivial shifts in the peak positions ($q_1\sim q_4$) with the addition of the G4.5 dendrimer show that the incorporation of dendrimers scarcely disturbs the lamellar periodicity of DDAB. So we suppose that the hydrophilic dendrimers are solubilized in the water domains and presumably adsorbed to one bilayer surface of DDAB, but do not penetrate into the DDAB bilayer. By eqs 1−3, the values of d_W, d_S, and a_S were calculated from the position (q_{max}) of the Bragg peaks

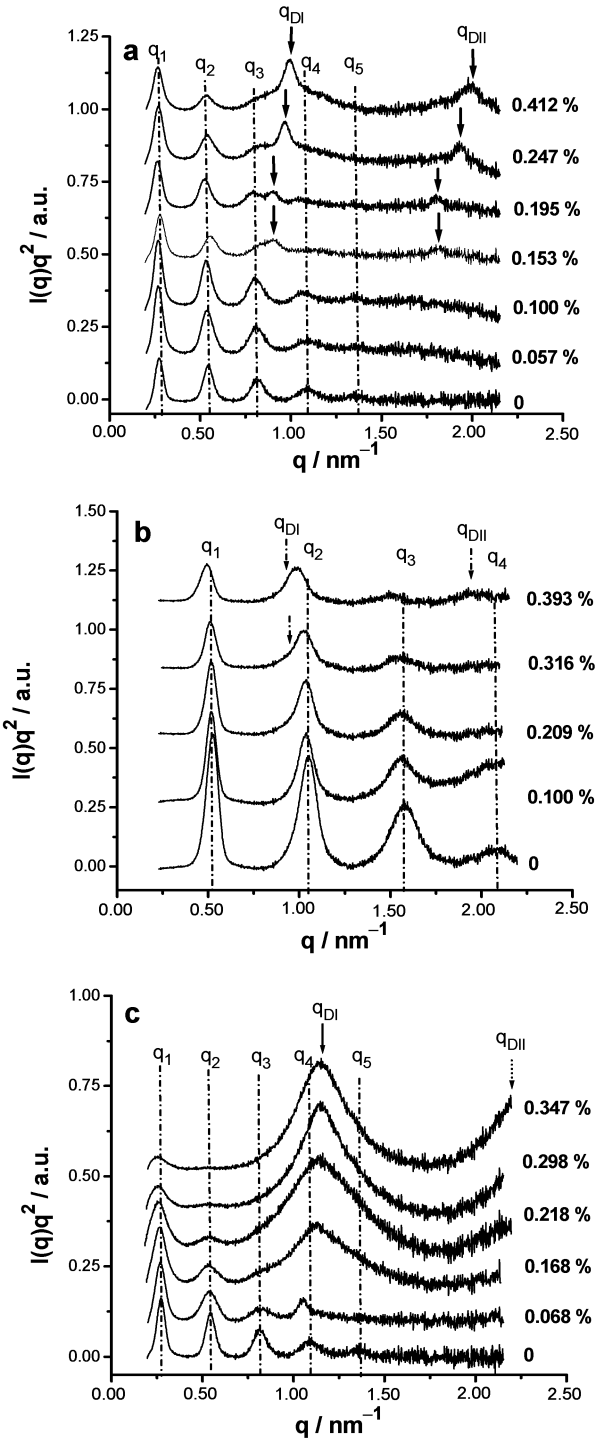

Figure 3. $I(q)q^2$ versus the scattering vector magnitude q curves with increasing the dendrimer concentration for different systems. (a) DDAB−G4.5−water at $W_S = 10\%$, (b) DDAB−G4.5-water at $W_S = 20\%$, (c) DDAB−G2.5−water at $W_S = 10\%$. The numbers represent the dendrimer concentration in wt %.

of two lamellar structures. These values are listed in Table 3 as a function of G4.5 concentration. The interlayer spacing values of the first and second lamellar structures are ∼23.5 and ∼6.7 nm, respectively. The cross-sectional area of the hydrophilic head of DDAB shows a constant value of 0.66 nm^2 with an increase in the G4.5 concentration, which is similar to that found in the DDAB−water system.

2. $W_S = 20\%$. Figure 3b shows X-ray patterns of the samples with increasing the dendrimer concentration from 0 to 0.4% at $W_S = 20\%$. Three peaks appear for all of the samples, indicating the formation of lamellar structures. The decrease in the intensity of these peaks indicates a decrease in the order of the lamellar periodicity due to the incorporation of dendrimers between DDAB bilayers. The second-order peak at $W_D = 0.316\%$ became broadened, and this is interpreted as the occurrence of the phase separation. A birefringent, transparent, and monophase lamellar structure was formed at $W_D < 0.316\%$. With the further addition of G4.5, the samples became turbid, suggesting the formation of hybrid structures.

The intensity of the second-order peak, like that of the first-order peak, decreases with increasing the G4.5 concentration from $W_D = 0$ to 0.316%. It remains constant in the range of $W_D = 0.316$ and 0.393%. It is obvious that a new peak appears at the q value near to the second-order peak. The overlapping of two peaks can be well separated by Gaussian fits (Figure 1b). The q_{DI} peak at 0.937 nm^{-1}, listed in Table 2, appears at $W_D = 0.393\%$, and the q_{DII} peak could be identified at 1.92 nm^{-1}, confirming the formation of a new lamellar structure. Then, the interlayer spacing of this new lamellar structure is found to be 6.7 nm, which is the same as that obtained from the system at $W_S = 10\%$. The interlayer spacing of the lamellar structure, the thicknesses of water domain and DDAB bilayer, and the cross-sectional area of the hydrophilic head of DDAB are listed in Table 3 for different G4.5 concentrations.

Lamellar Structures Containing the G2.5 Dendrimer at $W_S = 10\%$. To investigate the effect of dendrimer generation on the lamellar structures and interactions of dendrimers with oppositely charged surfactants, the G2.5 dendrimer at an early generation was added to the lamellar phase of DDAB. The $I(q)$-q^2 vs q plot for the system DDAB−G2.5−water at $W_S = 10\%$ is shown in Figure 3c. With an increase in the dendrimer concentration, the first-order and second-order peaks could be distinguished for the whole concentration range of dendrimer, and the third-order peak could be resolved unambiguously only at around $W_D = 0.068\%$, indicating the formation of a normal lamellar structure. The intensity of the first-order peak is considerably decreased when the dendrimer is added, and a broad peak is observed at high G2.5 concentrations ($\geq 0.168\%$). From the fit, a value of $q_{DI} = 1.11$ nm^{-1} is obtained, due to the formation of a new structure. The $I(q)q^2$ plot shown in Figure 3c also shows the existence of a second broad peak at $q_{DII} = 2.22$ nm^{-1}, with a ratio q_{DI}:q_{DII} = 1:2. According to the similar structure obtained for the systems containing the G4.5 dendrimer, we consider that the lamellar structure is also the most probable one for this system. One can then conclude that a monophase lamellar structure is formed at $W_D < 0.168\%$ and a two-phase lamellar structure appears at $W_D \geq 0.168\%$.

In Table 3 we show the interlayer spacings of two lamellar structures (d_1, d_{DI}), the thicknesses of the water domain (d_W) and of the DDAB layer (d_S), and the cross-sectional area of the hydrophilic head of DDAB (a_S), for the systems at different concentrations of the G2.5 dendrimer. The interlayer spacing of the first lamellar structure increases slightly from 23.4 to 25.2 nm, whereas the cross-sectional area of the hydrophilic head of DDAB decreases from 0.67 to 0.61 nm^2 with an increase in W_D up to 0.218%.

Lamellar Phase Transitions in the DDAB−Dendrimer−Water Systems. In this section we report phase separations that occur in our hybrid lamellar systems by the incorporation of dendrimers into the lamellar structures of DDAB. The addition of the G4.5 dendrimer resulted in the phase transition from a single-phase to a two-phase region. The critical dendrimer concentration (CDC) at the phase transition point increases with an increase in the DDAB concentration, as shown in Figure 5.

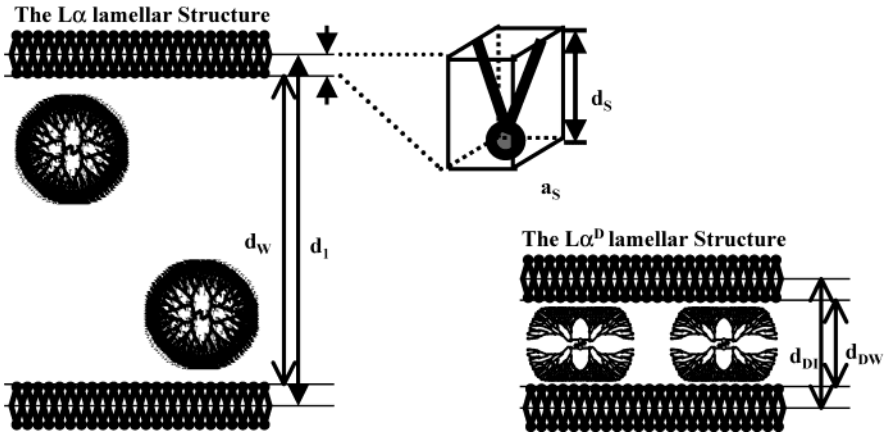

Figure 4. Schematic models of the lamellar L_α structure (left) and the lamellar L_α^D structure (right) for the interactions between anionic dendrimers and DDAB bilayers.

TABLE 2: Position, Area, Intensity, Width, and Domain Size of Gaussian Peaks of Lamellar Structures

		Gaussian peak q_1 of the L_α lamellar structure					Gaussian peak q_{DI} of the L_α^D lamellar structure				
W_D (wt %)	2[DDAB]/[−COONa]	position (nm^{-1})	area (nm^2)	intensity (a.u.)	FWHM (nm^{-1})	domain size (nm)	position (nm^{-1})	area (nm^2)	intensity (a.u.)	FWHM (nm^{-1})	domain size (nm)
G4.5-containing systems at W_S = 10 wt %											
0		0.271	0.0099	192.5	0.051	101					
0.057	154	0.265	0.0191	314.6	0.061	93					
0.100	88	0.264	0.0174	304.0	0.057	99					
0.153	58	0.274	0.0106	177.5	0.060	94	0.909	0.0004	4.3	0.095	59
0.195	45	0.260	0.0132	228.4	0.058	98	0.897	0.0005	5.6	0.094	60
0.247	35	0.265	0.0158	245.0	0.064	88	0.963	0.0012	12.7	0.091	63
0.412	21	0.262	0.0137	205.8	0.066	85	0.991	0.0018	15.9	0.115	49
G4.5-containing systems at W_S = 20 wt %											
0		0.518	0.0177	204.3	0.087	65					
0.100	175	0.513	0.0100	140.5	0.071	80					
0.209	84	0.511	0.0091	115.3	0.079	72					
0.316	55	0.508	0.0060	75.1	0.081	70	0.922	0.0004	2.5	0.178	32
0.393	44	0.487	0.0062	63.3	0.098	58	0.937	0.0008	4.2	0.193	29
G2.5-containing systems at W_S = 10 wt %											
0		0.268	0.0133	218.1	0.061	101					
0.068	125	0.264	0.0150	220.6	0.068	83					
0.168	50	0.258	0.0183	220.7	0.083	68	1.103	0.0041	10.6	0.386	15
0.218	38	0.249	0.0171	184.9	0.092	61	1.112	0.0063	17.3	0.365	16
0.298	28	0.248	0.0083	86.7	0.096	59	1.129	0.0065	20.1	0.326	17
0.347	24	0.248	0.0045	47.6	0.095	60	1.117	0.0081	21.5	0.376	15

A single lamellar phase was formed below the CDC line, and mixtures of two lamellar phases appeared above the CDC line. Compared with the high solubilizing capacity of lamellar structures of surfactants for linear polymers,[11] the corresponding solubilization for the dendrimers given by the CDC < 0.5% appears to be very low. The reason is likely the high hydrophilicity of the dendrimers that let them be solubilized in the water domains.

Discussion

Two Lamellar Structures. The ordered lamellar structure (L_α), which consists of DDAB bilayers and water domains, is formed at DDAB concentrations in the range of 4∼30%.[13,17] PAMAM dendrimers can be incorporated into the water domain between the DDAB bilayers below the CDC because of their small size and high water solubility.[14,18] The d_1 values of the lamellar structure were ∼23.4 nm for both G2.5 and G4.5 dendrimers at W_S = 10%, and 12.1 nm for the G4.5 dendrimer at W_S = 20%, remaining almost constant or increasing slightly with an increase in W_D. When the dendrimer concentrations surpass the CDC, new peaks, q_{DI} and q_{DII}, appear, indicating the formation of the second lamellar structure (see Figures 1 and 3). The d_{DI} values of the second lamellar structure are 6.7 nm for the G4.5 dendrimer at W_S = 10 and 20%, and 5.6 nm for the G2.5 dendrimer at W_S = 10%. Two lamellar structures with remarkably different interlayer spacings can be illustrated in Figure 4. The first lamellar structure, L_α, consists of a bilayer of DDAB and a domain of water, where PAMAM dendrimers are doped. The second lamellar structure, L_α^D, consists of a bilayer of DDAB and a dendrimer layer, which is sandwiched between the DDAB bilayers.

The thickness of the dendrimer layer (d_{DW}) is equal to the difference between the interlayer spacing of the L_α^D structure (d_{DI}) and the thickness of the DDAB bilayer ($2d_S$), i.e., $d_{DW} = d_{DI} - 2d_S$. The calculated d_{DW} values are 4.2 nm for the G4.5 dendrimer at W_S = 10 and 20% and 3.0 nm for the G2.5 dendrimer at W_S = 10% (Table 3). It is known that the dendrimer structure changes from a opened star structure with an asymmetric shape for the G2.5 dendrimer to a densely packed exterior structure with a nearly spherical shape for the G4.5 dendrimer.[4] Assuming dilute, noninteracting, and globular monodisperse particles, the dendrimer diameters, e.g., 5.9 nm (G4.5) and 3.8 nm (G2.5), were measured in 1% aqueous solutions by SAXS and calculated based on the Guinier approximation (the figures are not shown here). Those diameters of the dendrimer values are in good agreement with those shown

TABLE 3: Spacings of Lamellar Structures and Cross-Sectional Areas of Hydrophilic Heads of DDAB

W_S (wt%)	W_D (wt%)	W_W (wt%)	ϕ_S	d_1 (nm)	d_S (nm)	d_W (nm)	a_S (nm^2)	d_{DI} (nm)	d_{DW} (nm)
G4.5-containing systems at $W_S = 10$ wt %									
10.0	0	90.0	0.1033	23.4	1.2	21.0	0.67		
10.0	0.057	90.0	0.1030	23.6	1.2	21.1	0.66		
10.0	0.101	89.9	0.1033	23.8	1.2	21.3	0.65		
10.0	0.153	89.8	0.1033	23.4	1.2	21.0	0.66	6.9	4.5
10.0	0.195	89.8	0.1033	23.9	1.2	21.5	0.65	7.0	4.5
10.0	0.247	89.8	0.1032	23.4	1.2	21.0	0.66	6.5	4.1
10.0	0.412	89.6	0.1034	23.4	1.2	21.0	0.66	6.3	3.9
G4.5-containing systems at $W_S = 20$ wt %									
19.8	0	80.2	0.2036	12.1	1.2	9.7	0.65		
19.8	0.100	80.1	0.2034	12.3	1.2	9.8	0.64		
19.8	0.209	79.9	0.2043	12.3	1.3	9.8	0.64		
19.8	0.316	79.9	0.2036	12.4	1.3	9.9	0.63	6.8	4.3
19.8	0.393	79.8	0.2038	12.9	1.3	10.3	0.61	6.7	4.0
G2.5-containing systems at $W_S = 10$ wt %									
10.0	0	90.0	0.1033	23.4	1.2	21.0	0.67		
10.0	0.068	89.9	0.1033	23.8	1.2	21.3	0.65		
10.0	0.168	89.9	0.1028	24.4	1.3	21.8	0.64	5.7	3.2
10.0	0.218	89.8	0.1032	25.2	1.3	22.6	0.61	5.7	3.0
10.0	0.298	89.7	0.1032	25.3	1.3	22.7	0.61	5.6	2.9
10.0	0.347	89.7	0.1033	25.3	1.3	22.7	0.61	5.6	3.0

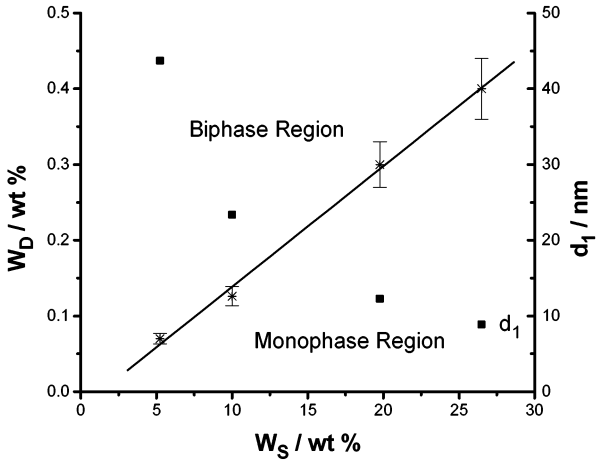

Figure 5. Phase diagram for the system DDAB−G4.5−water as a function of dendrimer concentration and DDAB concentration at 25 °C. In the figure, the corresponding d_1 values are plotted for the L_α structure. The standard error bar is estimated to be 10% of the corresponding CDC values.

in Table 1 and should be kept unchanged, as the dendrimer is doped in the water domains between the DDAB bilayers of the L_α structure. When the dendrimer concentration exceeds the CDC, the size of the dendrimer within two lamellar phases decreases from 5.9 nm (L_α) to 4.2 nm (L_α^D) for the G4.5 dendrimer and from 3.8 nm (L_α) to 3.0 nm (L_α^D) for the G2.5 dendrimer. The result above implies that a monolayer of collapsed dendrimers is tightly adsorbed between the surfactant bilayers.

Interactions of Doped Dendrimers with DDAB Bilayers. The most interesting results obtained in this investigation are concerned with the interactions of the cationic surfactant, DDAB, with the dendrimers at different generations. With the addition of dendrimers into the L_α structure, the dendrimers are doped inside the water domains and leave the bilayer thickness d_S unchanged. The slight change in d_1 and a_S with an increase in W_D, shown in Table 3, results from the strong electrostatic interactions between the terminal groups of dendrimers and the DDAB bilayers.

As seen in Figure 2, with decreasing the DDAB concentration from 30 to 4%, the interlayer spacing of the L_α structure increases, and then the thickness of water domain increases from 6 to 60 nm. It is expected that the CDC at low DDAB concentrations should be larger, due to a larger water domain, for the incorporation of dendrimers. However, the observed CDC of G4.5 dendrimer, contrary to the expectation, is almost proportional to the DDAB concentration that determines the amount of the DDAB bilayer, as shown in Figure 5. This linear relationship implies that the [DDAB]/[G4.5] ratio remains almost constant along the CDC line with an increase in the DDAB concentration, although the total volume fraction of water domains is decreased. This constant ratio is in agreement with the picture where parts of the terminal groups of the doped dendrimers adsorb and interact with the DDAB hydrophilic heads, as shown in Figure 4 (left).

Along the phase transition shown in Figure 5, the reciprocal of the slope of the CDC line is found to be 0.627. Taking into account this value and the molecular weights of the G4.5 dendrimer (26 258) and DDAB (462), one can calculate the [DDAB]/[G4.5] ratio as 3560 and the 2[DDAB]/[−COONa] ratio as 56 along this CDC line (notice that for the sake of simplicity the [−COONa]/2 is assumed to be equal to the half of the molar concentration of the dendrimer surface group). This ratio results from the strong interactions between the −COONa group and the oppositely charged surfactant DDAB, which limit the doping of dendrimers in the L_α structure and then induce the phase transition from L_α to L_α^D for further incorporation of dendrimers, when the dendrimer concentration exceeds the CDC.

A similar result was obtained for the system containing the G2.5 dendrimer (molecular weight 6267). The CDC of G2.5 dendrimer was 0.135% at $W_S = 10\%$. From this value, one can get the [DDAB]/[G2.5] ratio of 1000, and then the 2[DDAB]/[−COONa] ratio will be 62. As compared with G4.5, the similar 2[DDAB]/[−COONa] ratios imply that the electrostatic interactions between the −COONa groups and the DDAB bilayers mainly determine the CDC in the L_α structure.

Order of the L_α^D Structure. Above the CDC, the dendrimers are accumulated and assembled into a dendrimer layer sandwiched tightly between the DDAB bilayers, as illustrated in Figure 4 (right). The increase in the intensity of q_{DI} peaks, as shown in Table 2, indicates an increase in the orderliness of the L_α^D structure, when the G4.5 dendrimer concentration increases from 0.153 to 0.412% at $W_S = 10\%$ and from 0.316

to 0.393% at $W_S = 20\%$. The distance between the terminal groups of dendrimers can be used to explain the result obtained above. The separations between terminal groups for the 0.5∼3.5-generation dendrimers are all 1.2 nm, whereas the distance changes to 1.0 nm at the 4.5 generation and then linearly decreases with the dendrimer generation.[1,4,18] The average separation between the headgroups of DDAB, for comparison, is estimated to be 0.8 nm ($\approx a_S^{1/2}$). For the L_α^D structure, the distance between the terminal groups of the dendrimers comparable to the average separation between the headgroups of DDAB is favorable, because adjacent surfactants can better "enjoy" stabilizing hydrophobic interactions, resulting from greater intimacy of the surfactant hydrocarbon chains. The large size of the dendrimers may be favorable, because the "flattening" of the "curvature" of the dendrimer surface with increasing size should allow less distortion of the surfactant chains of bilayers, as their chains attempt to maximize the stabilization. A combination of the smaller distance between terminal groups and the flattening surface of the G4.5 dendrimer induces cooperative electrostatic interactions[1,3] of dendrimers with the DDAB bilayer, which favor the formation of the ordered L_α^D structure. Thus, the more dendrimers are adsorbed inside the liquid crystals, the higher the order of the L_α^D lamellar structure would become.

For the G2.5 dendrimer at $W_D = 0.168$∼0.347%, the very broad peaks of the L_α^D structure were observed at the same q value ($= 1.11$ nm^{-1}). The intensity of the broad peaks slightly increased and that of the first-order peak of the L_α structure, on the other hand, decreased considerably at $W_D > 0.168\%$. This could be explained from the small size of the G2.5 dendrimer and the large separation between the terminal groups, which cause ineffective cooperative adsorption on the surfactant bilayer.[1,3,11] The other possible reason is related to the flexibility of dendrimer structure. The G2.5 dendrimer, at a low generation, is more flexible than the G4.5 dendrimer, and it easily changes its shape after the incorporation between the bilayers of DDAB. The DDAB bilayers are only slightly distorted, and then the interlayer spacing of the lamellar structure and the cross-sectional area of the hydrophilic head of DDAB, as shown in Table 3, change slightly with increasing the G2.5 concentration. Then, the L_α^D lamellar structure becomes less ordered and a broadening of the peaks (with a decrease in the domain size) is observed. This is discussed further in the following section.

Domain Sizes of Lamellar Structures. The domain sizes of liquid crystals obtained in this study are in the range 15∼100 nm and were derived, as it was explained before, from the broadening of the diffraction peaks. The broadening of the diffraction peaks occurs from three different factors including (1) the instrumental resolution function, (2) the imperfections of the lattice, and (3) the finite size of the liquid crystals.[16] For our results, analyzed as to give a semiquantitative comparison within this study only, we neglected the broadening due to the contributions 1 and 2. This will be explained by the following.[16,19] (1) The instrumental resolution function was characterized by a beam image with a fwhm of 0.035 nm^{-1}, 1.5 times narrower than the smallest measured fwhm of the Bragg peaks. (2) There are two general types of lattice imperfections to be considered, but only the so-called second-kind imperfection contributes to the line broadening. This imperfection does not contribute much to the peak broadening in the present work, because the liquid crystalline domains contain only a small amount of unit cells. Therefore, the main changes in the line broadening are due to the changes in the finite size of the liquid crystals.

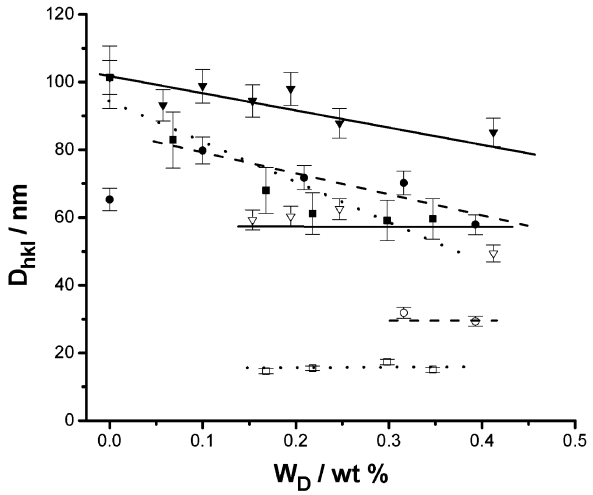

Figure 6. Domain sizes of two lamellar structures (L_α and L_α^D) versus dendrimer concentration for different systems. (▼, ▽) DDAB 10% + G4.5; (●, ○) DDAB 20% + G4.5; (■, □) DDAB 10% + G2.5; closed symbols, L_α; open symbols, L_α^D. The standard error bar is estimated to be 5% of the corresponding D_{hkl} values.

Upon increasing the incorporation of dendrimers into the water domain between the DDAB bilayers, the single lamellar structure changes into the mixture of two lamellar structures. The calculated domain sizes, D_{hkl}, for both structures are shown in Figure 6 for dendrimers-containing L_α structures at $W_S = 10$ and 20%. The domain size for the first lamellar structure, which ranges between 60∼100 nm, generally decreases with increasing the dendrimer concentration for G4.5 and G2.5 dendrimer-containing systems. Unlike the L_α structure, the domain size of the L_α^D structure remains almost constant. For example, the D_{hkl} values are 60 and 30 nm for G4.5-containing systems at $W_S = 10$ and 20%, respectively, and 15 nm for a G2.5-containing system at $W_S = 10\%$.

In the case of the L_α structure, the DDAB bilayer mainly decides the domain size, whereas the dendrimers doped only disturb the ordered structure of DDAB. It is then supposed that the L_α structure formed with DDAB alone has the biggest domain size. With the incorporation of dendrimers into the water domain, the ordered bilayer is distorted and its domain size decreases, due to the cross-linking of adjacent bilayers through electrostatic bilayer−dendrimer stacking, a kind of flocculation process, for all systems containing dendrimers examined here (Figure 6). For the G4.5 dendrimer at $W_S = 10$ and 20%, the influence of the addition of dendrimers in the L_α structure is almost the same because the linear relationships of the domain size, as a function of dendrimer concentration, show almost the same slopes in two systems (see Figure 6). For the G2.5 dendrimer at $W_S = 10\%$, on the other hand, the domain size decreases considerably from ca. 100 nm at $W_D = 0\%$ to 60 nm at $W_D = 0.347\%$. The reason for the bigger drop in D_{hkl} for the G2.5 dendrimer may be due to the increased adsorption of dendrimers (corresponding to the lower 2[DDAB]/[−COONa] ratios at the same dendrimer concentration shown in Table 2) as well as the larger separation between the terminal carboxylate groups, as compared with the G4.5 dendrimer.

The domain size of the L_α^D structure remains almost constant with increasing the dendrimer concentration, whereas the volume fraction of the L_α^D phase is increased with the increase in the intensity of the q_{DI} peaks. By increasing the dendrimer concentration, the L_α structure is turned into the $L_\alpha + L_\alpha^D$ structures above the CDC, where the phase transition $L_\alpha \Leftrightarrow L_\alpha^D$ reaches equilibrium. The new L_α^D structure formed consists of

a fixed composition of DDAB and dendrimer, which mainly determine the domain size of the L_α^D structure. In addition, the L_α^D structure is generated from the L_α structure with the further addition of dendrimers. So the domain size of the L_α^D structure decreases from 60 nm at $W_S = 10\%$ to 30 nm at $W_S = 20\%$ for the G4.5 dendrimer, because the L_α structure at a low W_S has a larger domain size. Moreover, the domain size for the G2.5 dendrimer is smaller than that for the G4.5 dendrimer at the same W_S, due to the difference in their structural properties as it was discussed before. The domain size of L_α^D is generally small and contains only a few stacks because of the strong repulsion interactions between the dendrimer molecules.

Conclusions

The lamellar structures of the cationic surfactant DDAB with anionic PAMAM dendrimers were investigated by SAXS at 25 °C. The incorporation of dendrimers with the half-generations (G2.5, G4.5) into the lamellar liquid crystal of DDAB resulted in the phase transition from a single lamellar structure to a biphase lamellar structure at the critical dendrimer concentration (CDC), corresponding to the critical [DDAB]/[Gn.5] ratios of 3560 (G4.5) and 1000 (G2.5). The similar 2[DDAB]/[−COONa] ratios, 56 for the G4.5 and 62 for the G2.5 dendrimer-containing systems at $W_S = 10\%$, result from the electrostatic interactions between the terminal groups of dendrimers and the bilayers of DDAB.

The SAXS measurements revealed lamellar structures (L_α and L_α^D) and interactions of dendrimers with DDAB, which change as a function of dendrimer concentration and generation. The L_α structure consists of bilayers of DDAB and dendrimer molecules doped into the aqueous domain of the lamellar phase. The L_α^D structure contains collapsed dendrimer monolayers sandwiched between DDAB bilayers. The dendrimer layer thickness was found to be 4.2 nm for the G4.5 dendrimer and 3.0 nm for the G2.5 dendrimer. Gaussian fits of SAXS diffraction patterns indicate that the G4.5 dendrimer can form an ordered L_α^D structure with larger domain sizes, as compared with the G2.5 dendrimer.

Acknowledgment. This work was financially supported by the Mitsubishi Foundation and by Grant-in-Aid for Scientific Research No. 11650928 from the Ministry of Education, Science and Culture, Japan.

References and Notes

(1) Caminati, N. J.; Turro, N. J.; Tomalia, D. A. *J. Am. Chem. Soc.* **1990**, *112*, 8515.
(2) Gopidas, K. R.; Leheny, A. R.; Caminati N. J.; Turro, N. J.; Tomalia, D. A. *J. Am. Chem. Soc.* **1991**, *113*, 7335.
(3) Ottaviani, M. F.; Turro, N. J.; Jockusch, S.; Tomalia, D. A. *J. Phys. Chem. B* **1996**, *100*, 13675.
(4) Ottaviani, M. F.; Andechaga, P.; Turro, N. J.; Tomalia, D. A. *J. Phys. Chem. B* **1997**, *101*, 6057.
(5) Ottaviani, M. F.; Matteini, P.; Brustolon, M.; Turro, N. J.; Jockusch, S.; Tomalia, D. A. *J. Phys. Chem. B* **1998**, *102*, 6029.
(6) Li, Y.; McMillan, C. A.; Bloor, D. M.; Penfold, J.; Warr, J.; Holzwarth, J. F.; Wyn-Jones, E. *Langmuir* **2001**, *16*, 7999.
(7) Friberg, S. E.; Podzimek M.; Tomalia, D. A.; Hedstrand, D. M. *Mol. Cryst. Liq. Cryst.* **1988**, *164*, 157.
(8) Baars, M. W. P. L.; van Boxtel, M. C. W.; Bastiaansen, C. W. M.; Broer, D. J.; Sontjens, S. H. M.; Meijer, E. W. *Adv. Mater.* **2000**, *12*, 715.
(9) Yeh, F.; Sokolov, E. L.; Khokhlov, A. R.; Chu, B. *J. Am. Chem. Soc.* **1996**, *118*, 6615.
(10) Radler, J. O.; Koltover, I.; Salditt, T.; Safinya, C. R. *Science* **1997**, *275*, 810.
(11) Porcar, L.; Marignan, J.; Ligoure, C.; Gulik-Krzywicki, T. *Langmuir* **2000**, *16*, 2581.
(12) Tomalia, D. A.; Naylor, A. M.; Goddard, W. A. *Angew. Chem., Int. Ed. Engl.* **1990**, *29*, 138.
(13) Kunieda, H.; Shigeta, K.; Ozawa, K. *J. Phys. Chem. B* **1997**, *101*, 7952.
(14) Prosa, T. J.; Bauer, B. J.; Amis, E. J.; Tomalia, D. A.; Scherrenberg, R. *J. Polym. Sci. Part B: Polym. Phys.* **1997**, *35*, 2913.
(15) Li, X.; Kunieda, H. *Langmuir* **2000**, *16*, 10092.
(16) (a) International Union of Crystallography. *International Tables for X-ray Crystallography*; Dordrecht: Holland, 1985; Part III, pp 318−323. (b) Kumar, A.; Kunieda, H.; Vazquez, C.; López-Quintela, M. A. *Langmuir* **2001**, *17*, 7245.
(17) Marques, E. F.; Regev, O.; Edlund, H.; Khan, A. *Langmuir* **2000**, *16*, 8255.
(18) Prosa, T. J.; Bauer, B. J.; Amis, E. J. *Macromolecules* **2001**, *34*, 4897.
(19) Als-Nielsen, J.; Lister, J. D.; Birgeneau, R. J.; Kaplan, M.; Safinya, C. R.; Lindegaard-Andersen, A.; Mathiesen, S. *Phys. Rev. B* **1980**, *22*, 312.